Journal of Hazardous Materials Advances 5 (2022) 100046

Contents lists available at ScienceDirect

Journal of Hazardous Materials Advances

journal homepage: www.elsevier.com/locate/hazadv

Three-dimensional excitation-emission matrix (EEM) fluorescence approach to probing the binding interactions of polystyrene microplastics to bisphenol A

Yu-Ying Zhu[a,1], Yang Liu[a,1], Juan Xu[a,*], Bing-Jie Ni[b]

[a] Shanghai Key Lab for Urban Ecological Processes and Eco-Restoration, Shanghai Organic Solid Wastes Biotransformation Engineering Technical Research Center, School of Ecological and Environmental Sciences, East China Normal University, Shanghai 200241, China
[b] Centre for Technology in Water and Wastewater, School of Civil and Environmental Engineering, University of Technology Sydney, Sydney, NSW 2007, Australia

ARTICLE INFO

Keywords:
Microplastics
Bisphenol A
Interaction
Three-dimensional excitation-emission matrix fluorescence

ABSTRACT

Microplastics (MPs) are readily to bind with contaminants, hence becoming the mobile composite pollutions with the migration of MPs in the environment. However, the binding mechanisms between MPs and various contaminants are still unclear due to the scarcity of investigation methods. In this work, three-dimensional excitation-emission matrix fluorescence spectroscopy approach is developed to probe the binding interactions between polystyrene MPs and a typical hydrophobic comtaminant bisphenol A (BPA). The binding affinity and thermodynamic parameters of the binding interactions are accurately and rapidly determined. Roles of environmental conditions in the binding interactions of MPs and BPA are discriminated. Results show that the binding strength of MPs to BPA is relatively higher under neutral (logK=4.96, pH 7) and weak acidic (logK=4.63, pH 6) conditions. The binding strength significantly grows with the increasing temperature from 4 to 35 °C. The binding process is barely influenced by ionic strength, but being promoted in the presence of divalent ions (Ca^{2+} and Mg^{2+}). The binding process of MPs to BPA is solely driven by entropy. Under neutral condition, hydrophobic forces dominate the binding interactions between MPs and BPA, with the assistance of weak hydrogen bonds. The predominant hydrophobic interactions are weakened under acidic conditions, resulting in lower binding strength. Under alkaline conditions, both hydrophobic forces and hydrogen bonds are weakened, while electrostatic repulsions are magnified, leading to the obviously decreased binding strength. The results benefit to a better understanding of the composition pollutions of MPs and hydrophobic pollutants in aquatic environments.

1. Introduction

Bisphenol A (BPA) is a frequently-used plasticizer, which is ubiquitously detected in the environment due to the massive emissions from plastic industry. BPA is demonstrated to be an endocrine disrupting chemical, exerting negative influences on male reproductive function and child neurodevelopment (Jiang et al., 2019). The plastics carrying with BPA migrate in the environment, becoming mobile BPA pollution sources. Recent studies demonstrate that microplastics (MPs) are important sources of BPA entering the aquatic environments (Liu et al., 2019).

MPs, plastic fragments whose diameter are less than 5 mm, have attracted global attentions for their adverse environental impacts (Liu and Wang 2020, Luo et al., 2022). MPs in the environment are classified into two categories, primary MPs and secondary MPs. Primary MPs generally originate from industrial production and personal cleaning products, such as resin particles, facial cleansers, toothpastes and body wash (Auta et al., 2017). These large plastic debris (primary MPs) can be further degraded or broken into secondary MPs during the physical, chemical and biological processes, i.e. aging and weathering processes. Owning to the small particle size and large specific surface area, MPs are more readily to accumulate the pollutants than the common plastic debris (Liu et al., 2021). Once BPA carried MPs are ingested by aquatic organisms, both MPs and the adsorbed BPA will be harmful to the food web, even the entire ecosystem (Lei et al., 2018). Therefore, it is necessary to systematically explore the binding interactions between MPs and BPA.

The characteristics of MPs (plastic types, color, size, crystallinity and so on) determine their binding capacity to various pollutants (Guo et al., 2012). The adsorption level of perfluorooctanesulfonamide onto MPs of polyethylene, polystyrene and polyvinyl chloride are higher than that of perfluorooctanesulfonat (Wang et al., 2015). Polyethylene MPs gather contaminants such as pyrene and phenanthrene more easily compared to polystyrene and polyvinylchloride MPs (Wang and Wang 2018).

* Corresponding author.
E-mail address: jxu@des.ecnu.edu.cn (J. Xu).
[1] These authors contributed equally to this work.

https://doi.org/10.1016/j.hazadv.2022.100046
Received 8 November 2021; Received in revised form 20 December 2021; Accepted 5 January 2022

Discolored MPs are able to adsorb more polychlorinated biphenyls than MPs without discoloration (Wang et al., 2018). In addition, environmental conditions significantly govern the binding interactions between MPs and pollutants. For example, the adsorption capacities of polystyrene plastics to tylosin tartrate and sulfamethazine highly depend on the aging degree of plastics (Ding et al., 2020). Alkaline conditions weaken the binding affinity of polypropylene and polystyrene MPs to 9-nitroanthrene (Zhang et al., 2020). Increasing temperature from 298 to 318 K promotes the adsorption of polyethylene MPs to pesticides such as Carbendazim, Malathion and Diflubenzuron (Wang et al., 2020). Therefore, to illuminate the binding behaviors of MPs to diverse pollutants, it is necessary to explore the fundamental mechanisms that driven the binding process, i.e. thermodynamics.

In this study, three-dimensional excitation-emission matrix (3D-EEM) fluorescence spectroscopy (Yu et al., 2020b), was applied to investigate the binding interactions between polystyrene MPs and BPA. Polystyrene, usually processes into disposable foam lunch boxes, is the principal category of MPs (Engler 2012). Influences of environmental conditions, including pH value, ionic strength, temperature and divalent metal ions on the binding interactions were explored. To reveal the mechanisms driving the binding processes of MPs to BPA, thermodynamic parameters including Gibbs free energy change (ΔG), enthalpy change (ΔH) and entropy change (ΔS) of the binding interactions were determined. Our work aims to develop a universal approach that can rapidly and accurately probe the binding process of MPs to organic pollutants such as BPA. The results benefit to a better understanding of the composite pollution of MPs and organic pollutants in aquatic environments.

2. Materials and methods

2.1. Chemicals

Polystyrene MPs solution (100 nm, 2.5% w/v) and BPA were purchased from Aladdin Co. Ltd (Shanghai, China). The other reagents were from Sinopharm Chemical Reagent Co., Ltd (Shanghai, China).

2.2. Binding experiments of MPs to BPA

The binding experiments were conducted under different environmental conditions, including pH (4–10), ionic strength (10–500 mM), temperatures (4, 25, 35 ˚C). Phosphate buffer (PBS) was used as the solvent. The tubes were filled with MPs solutions (250 mg/L) of the same volume and BPA solutions (95 mg/L) of gradient volumes. Then, PBS was added into each tube to maintain a total volume of 10 mL. The final concentrations of MPs solutions were 7.5 mg/L, while BPA concentrations were in the range of 0–13.3 mg/L. Afterwards, the solutions were mixed using an oscillator and balanced for 4 h in a temperature-controlled incubator before analysis.

To investigate the influence of divalent ions on the binding interactions, pure water was used as solvent to avoid precipitation. Divalent metal ions (1 mM $MgCl_2$ or 1 mM $CaCl_2$) were added into the tubes in addition to MPs and BPA. The final concentrations of MPs solutions were adjusted to 4.95 mg/L. The other steps were the same as those described above.

2.3. Samples analysis

3D-EEM spectra were measured with a luminescence spectrometer (F-4600, Hitachi Co., Japan). The excitation wavelength changed from 200 to 400 nm at 5 nm increments, and the emission wavelength was from 280 to 550 nm at 0.5 nm increments. The excitation and emission slits were set at 5 nm, and the scanning speed was 2400 nm/min. Since the spectra of MPs overlapped with that of BPA, the obtained EEM data was processed by parallel factor analysis (PARAFAC) with DOMFluorv1.7 toolbox. Then, the evolution of the fluorescence intensity score of the MPs after binding with BPA were resolved. The details were described in our previous studies (Gan et al., 2019, Yan et al., 2019). Then, the binding constants and binding sites were calculated using the double logarithmic equation (Yan et al., 2019).

$$\log \frac{F_0 - F}{F} = \log K + n \log[Q] \quad (1)$$

Where F_0 is the initial fluorescence intensity score of MPs based on PARAFAC analysis, F is the fluorescence intensity score of MPs in the presence of BPA whose concentration is [Q], n is the number of binding sites, and K is the binding constant.

Zeta potential of MPs before and after binding with BPA was measured in triplicate on a zeta potential analyzer (NANO ZS3600, Malvern Co., UK) at 25 ˚C.

3. Results and discussion

3.1. Evolution of 3D-EEM spectrum of MPs interacted with BPA

The binding interactions between MPs and BPA were investigated by 3D-EEM fluorescence quenching combined with PARAFAC analysis. Apparently, the 3D-EEM spectra of MPs (Fig. 1a) changed with the addition of BPA (Fig. 1b) due to the binding interactions. PARAFAC analysis was introduced to resolve the overlapped 3D-EEM spectra, and two components were extracted: MPs in Fig. 1c (Ex/Em = 220/330 nm, Ex/Em = 260/330 nm), and BPA in Fig. 1d (Ex/Em = 230/310 nm, Ex/Em = 275/310 nm). When gradient concentrations of BPA were added, the EEM spectrum of MPs evolved regularly (Fig. 2a–h). The peak intensities related to MPs decreased, while the ones ascribed to BPA climbed. Based on PARAFAC analysis, it was found that the fluorescence intensity score of MPs decreased with the increasing BPA concentration (Fig. 2i), following the double logarithmic equation well.

3.2. Thermodynamic mechanisms driving the binding of MPs to BPA influenced by pHs

The binding interactions between BPA and MPs are highly dependent on solution pHs. The maximum value of logK was obtained at pH 7 (Table 1), indicating the binding affinity of MPs to BPA was the highest under the neutral condition.

The binding affinity between MPs and BPA monotonically increased with the elevated pH value from 4 to 7 (Table 1). Due to the instinct hydrophobicity of BPA and polystyrene MPs, hydrophobic interactions primarily drove the binding process of MPs to BPA. The high surface/volume ratio of polystyrene MPs provided abundant active sites for the retention of hydrophobic contaminants (Liu et al., 2016). MPs were negatively charged in the pH range of 4–7 (Fig. 3), and the weak electrostatic repulsion maintained the uniform dispersion of the MPs. With the declined pH value, the negative charges of MPs reduced. The weakened electrostatic repulsion induced the aggregation of MPs, leading to the decreased hydrophobic sites of MPs for BPA to combine with. Therefore, the hydrophobic interactions between MPs and BPA were more significant at pH 7. In addition to hydrophobic interactions, electrostatic forces were also involved in the binding interactions. Solution pH altered both the charges on MPs surface and the charges carried by BPA molecules, hence impacting the electrostatic repulsions between MPs and BPA. Fig. 3a showed that zeta potential of MPs gradually decreased when pH increased from acidic to neutral. Especially, when pH varied from 5 to 6, the absolute value of zeta potential significantly improved from 8.0 to 27.5 mV, indicating that negative charges of MPs augmented as pH went up to neutral. The speciation of BPA was also highly dependent on solution pHs. The chemical equilibrium equations of BPA in water could be described as (Eqs. (2)-(9)):

$$Bis(OH)_2 \Leftrightarrow Bis(OH)(O)^- + H^+,\ K_{a1} = [Bis(OH)(O)^-][H^+]/[Bis(OH)_2] \quad (2)$$

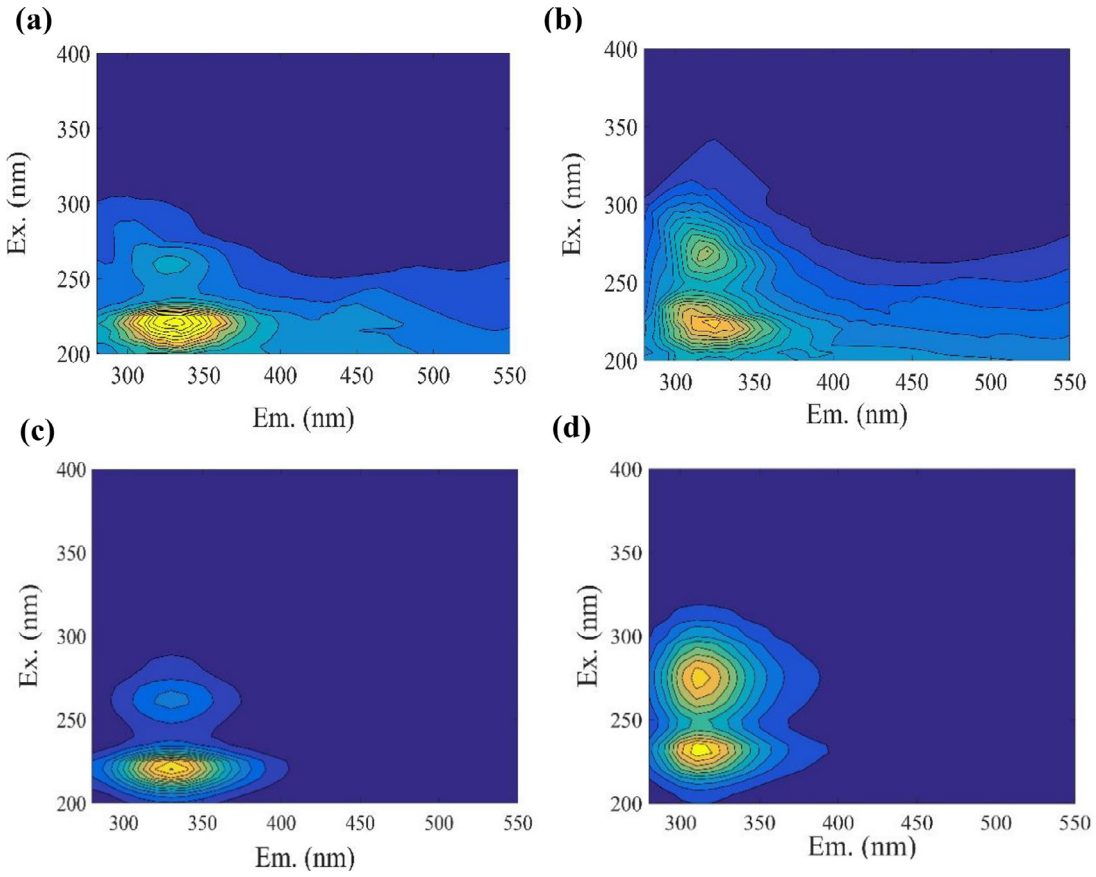

Fig. 1. EEM fluorescence spectra of (a) MPs and (b) mixture of MPs and BPA, the individual component of (b) by PARAFAC analysis: (c) MPs, (d) BPA.

Table 1
Binding constants (logK) and binding sites (*n*) of the interactions between MPs and BPA under different environmental conditions.

Factors		logK	n	R^2 [a]
pH	4	3.12±0.31	0.78±0.097	0.9891
(ionic strength	5	3.98±0.038	1.00±0.0090	0.8448
50 mM, 25 °C)	6	4.63±0.076	1.09±0.017	0.9637
	7	4.96±0.024	1.25±0.0050	0.9644
	8	4.10±0.12	1.02±0.011	0.9829
	9	4.00±0.067	0.96±0.017	0.9068
	10	3.19±0.22	0.77±0.050	0.9591
Ionic strength	10 mM	4.52±0.049	1.08±0.032	0.9971
(pH 7, 25 °C)	100 mM	4.40±0.10	1.00±0.029	0.9694
	250 mM	4.38±0.15	1.04±0.033	0.9924
	500 mM	4.47±0.17	1.10±0.048	0.9830
Divalent metal ions	Pure water	2.57±0.084	0.70±0.015	0.9792
(pH 7, 25 °C)	Mg^{2+} (1 mM)	2.67±0.083	0.74±0.021	0.8261
	Ca^{2+} (1 mM)	3.33±0.19	0.88±0.035	0.9929

[a] The correlation coefficient fitted by Eq. (1).

$$Bis(OH)(O)^- \Leftrightarrow Bis(O_2)^{2-} + H^+,\ K_{a2} = [Bis(O_2)^{2-}][H^+]/[Bis(OH)(O)^-] \quad (3)$$

Accordingly, the pK_a values of BPA are calculated as follows (Escalona et al., 2014):

$$pK_{a1} = -lg([Bis(OH)(O)^-]) - lg([H^+]) + lg([Bis(OH)_2]) = 9.6 \quad (4)$$

$$pK_{a2} = -lg([Bis(O_2)^{2-}]) - lg([H^+]) + lg([Bis(OH)(O)^-]) = 10.2 \quad (5)$$

The ratio of three BPA speciation follows:

$$\Delta[Bis(OH)_2] + \Delta[Bis(OH)(O)^-] + \Delta[Bis(O_2)^{2-}]=1 \quad (6)$$

Combining (4)-(6), the ratio of three BPA speciations with pH:

$$\Delta[Bis(OH)_2] = 10^{19.8-2pH}/(1 + 10^{10.2-pH} + 10^{19.8-2pH}) \quad (7)$$

$$\Delta[Bis(OH)(O)^-] = 10^{10.2-pH}/(1 + 10^{10.2-pH} + 10^{19.8-2pH}) \quad (8)$$

$$\Delta[Bis(O_2)^{2-}] = 1/(1 + 10^{10.2-pH} + 10^{19.8-2pH}) \quad (9)$$

As shown in Fig. 4, BPA basically presented in the molecule form of $Bis(OH)_2$ over the pH range from 4 to 7. Therefore, the electrostatic interactions were not the dominant mechanisms for the binding interactions between BPA and MPs over the pH range of 4–7.

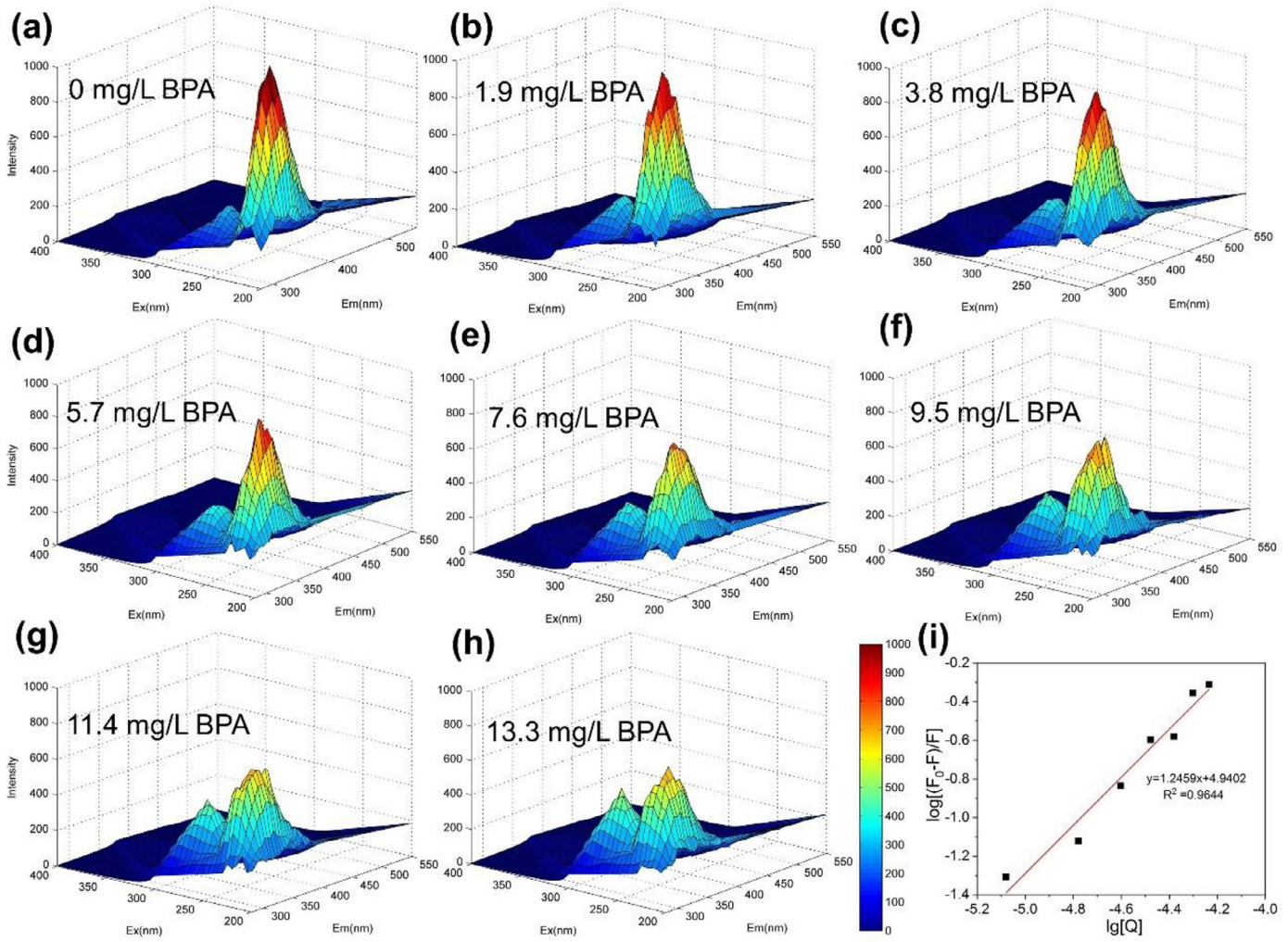

Fig. 2. Evolutions in EEM spectrum of MPs with the increasing dosage of BPA (a–h), and (i) the fitting results of fluorescence score obtained from PARAFAC analysis (pH 7, ionic strength 50 mM, 25 ˚C).

BPA began to dissociate H^+ when pH value increased over 7, with the appearance of monovalent anion [Bis(OH)O^-] and dianion ($BisO_2^{2-}$) (Yan et al., 2019). The dissociation of BPA reduced hydrophobicity of BPA, resulting in the weakened hydrophobic interactions between BPA and MPs (Jin et al., 2018). At the same time, zeta potential of MPs slightly decreased with the increasing pH value (Fig. 3a). Consequently, the electrostatic repulsion was magnified with the increasing pH and impeded the binding process of BPA to MPs. The binding strength clearly declined with the increased solution pH value from 8 to 10.

Similar phenomenon of pH dependent interactions between MPs and contaminants were reported in other studies. For example, anionic perfluorooctanesulfonate was more readily to be adsorbed on polyethylene and polystyrene at low pH values due to the reduced electrostatic repulsion with the protonation of MPs surface (Wang et al., 2015). Alkaline conditions facilitated adsorption of metals (Cd, Co, Ni, and Pb) onto virgin and beached plastic pellets because of the improved coulombic interactions between metals and pellets (Holmes et al., 2014). The hydrogen bonds that dominated the combination of MPs and 17β-estradiol under acidic conditions were weakened with the increasing pH (Hu et al., 2020a). MPs got the maximum adsorption capacity to oxytetracycline at pH = 5. The adsorption capacity decreased when pH was over 7.32, mainly due to the magnified electrostatic repulsion between MPs and ionized oxytetracycline (Zhang et al., 2018a). Similar phenomenon was also reported for the interactions between MPs and triclosan (Li et al., 2019). However, the adsorption of non-ionic lubrication oil to nano-polyethylene or micro-polystyrene was irrelevant to solution pH (Hu et al., 2017).

In order to analyze the binding mechanisms between MPs and BPA under different pH conditions, thermodynamic parameters including ΔH and ΔS at pH 5, 7, and 9 were fitted by Van't Hoff equation (Gan et al., 2019).

$$\ln K = -\frac{\Delta H}{RT} + \frac{\Delta S}{R} \tag{10}$$

Where R is the gas constant (8.314 J/mol/K), T is thermodynamic temperature. The Gibbs free energy change (ΔG) was calculated as follows (Eq. (11)):

$$\Delta G = \Delta H - T\Delta S \tag{11}$$

As shown in Table 2, increasing temperature improved the binding strength between BPA and MPs regardless of solution pH, since the binding process was endothermic with the positive ΔH values. The adsorption of organic pollutants such as BPA by plastics was dominated by different mechanisms according to the properties of pollutants, plastics and environmental conditions. For example, the adsorption of BPA onto polypropylene nonwoven resulted from hydrophobic interactions and hydrogen bonding (Zhou et al., 2014). Adsorption of bisphenol analogues by polyvinyl chloride MPs were attributed to hydrophobic interactions, electrostatic interactions, and noncovalent binding (hydrogen and halogen bonds) (Wu et al., 2019). Generally, hydrophobic forces, electrostatic interaction, and noncovalent binding contributed

Table 2
Thermodynamic parameters of the interactions between MPs and BPA at various pH values (ionic strength 50 mM).

pH	T(°C)	logK	n	R_1^2 [a]	ΔG(kJ/mol)	ΔH(kJ/mol)	ΔS(J/mol/K)	-TΔS(kJ/mol)	R_2^2 [b]
5	4	3.68±0.059	0.96±0.021	0.8684	−19.17	44.79	230.76	−63.96	0.8240
	25	3.98±0.038	1.00±0.0090	0.8448	−24.01			−68.80	
	35	4.62±0.098	1.03±0.0090	0.9623	−26.32			−71.11	
7	4	3.79±0.18	0.80±0.0070	0.9392	−19.34	135.81	559.79	−155.15	0.9031
	25	4.96±0.024	1.25±0.0050	0.9644	−31.09			−166.90	
	35	6.56±0.040	1.31±0.020	0.9607	−36.69			−172.50	
9	4	3.22±0.11	0.80±0.032	0.6468	−16.85	72.90	323.84	−89.75	0.9683
	25	4.00±0.067	0.96±0.017	0.9068	−23.65			−96.55	
	35	4.66±0.022	1.10±0.0050	0.9512	−26.89			−99.79	

[a] The correlation coefficient fitted by Eq. (1).
[b] The correlation coefficient fitted by Eq. (10).

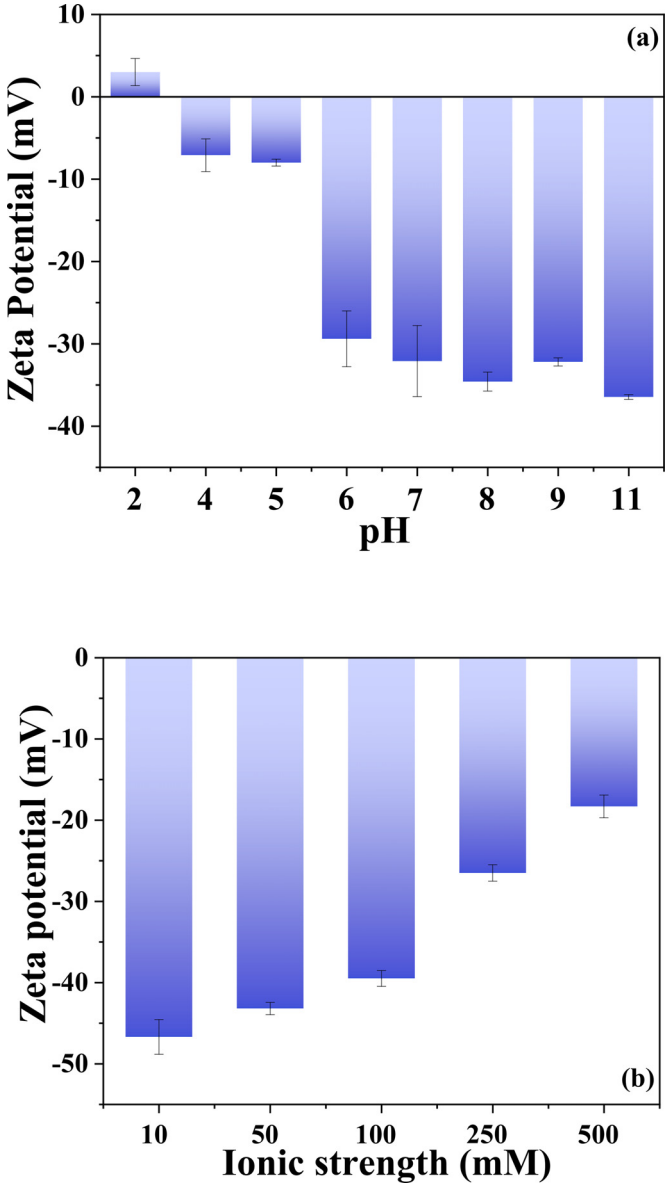

Fig. 3. Zeta potential of MPs under different (a) pH values and (b) ionic strengths.

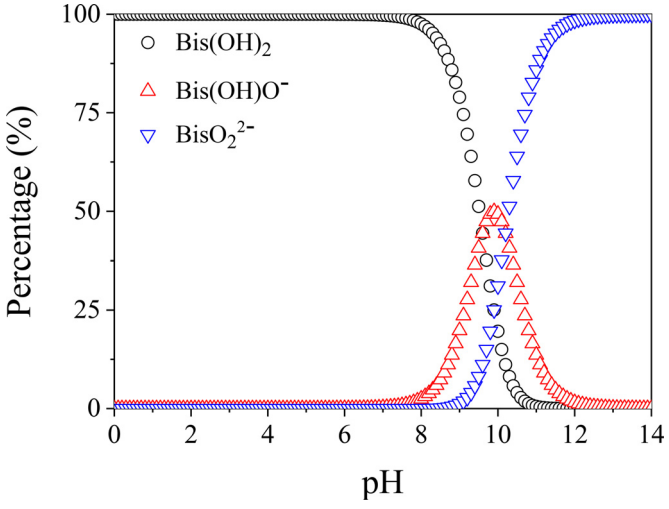

Fig. 4. Distribution of different species of BPA at various pH values.

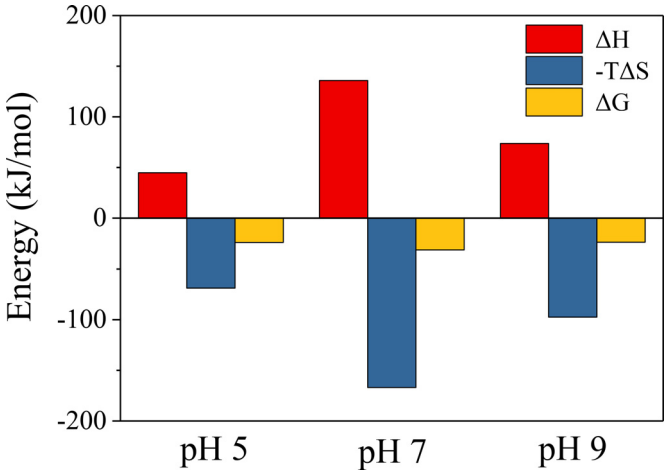

Fig. 5. Evolution of thermodynamic mechanisms driving BPA binding to MPs at different pH values (ionic strength 50 mM, 25 °C).

to the binding process of MPs and BPA. Different interaction mechanisms created different thermodynamic parameters (Ross and Subramanian 1981): hydrophobic force led to $\Delta H > 0$, $\Delta S > 0$, hydrogen bond induced $\Delta H < 0$, $\Delta S < 0$, electrostatic force generated $\Delta H \approx 0$ (slightly positive or negative), $\Delta S > 0$. The thermodynamic parameters displayed in Fig. 5 reflected the comprehensive results of different interaction mechanisms involved in the present work. The positive ΔH and negative -TΔS appeared at pH 5, 7 and 9, and negative ΔG demonstrated that the binding interactions could occur spontaneously. Positive ΔH did not facilitate the binding interactions, while negative -TΔS that contributed by hydrophobic force and electrostatic interaction triggered the binding interactions. That meant the binding process of BPA to MPs was solely driven by entropy, no matter under the acidic, neutral or alkaline conditions. However, the absolute values of the thermodynamic

parameters varied at different pH values, corresponding to the different binding extent.

At pH 7, the highest absolute values of ΔH, –TΔS, and ΔG were obtained (Table 2). Since BPA was in the molecular form at pH 7, the electrostatic interactions between BPA and MPs were insignificant. Considering that hydrogen bond would induce negative ΔH and positive -TΔS, hydrophobic interactions (positive ΔH, negative –TΔS) were more intensive at pH 7 compared to those at pH 5 and 9. Weak hydrogen bonds could form between alkyl groups of polystyrene (H donor) and aromatic rings of BPA (H acceptor) (Wu et al., 2019). These intermolecular hydrogen bonds of MPs-BPA complex were readily broken with the growing temperature. Thus, when the temperature rose, noncovalent binding strength of BPA-MPs complex were reduced. In summary, hydrophobic forces dominated the binding interactions between MPs and BPA under the neural condition, with the assistance of weak hydrogen bonds.

At pH 5, hydrophobic interactions between MPs and BPA were still predominant, and electrostatic interactions were minor. However, the absolute values of ΔH and –TΔS decreased, which was offset by the increased hydrogen bonds (negative ΔH, positive –TΔS) under acidic conditions. Non dissociated species of BPA were favorable for H-bonding interactions (Yang et al., 2008). The hydrogen bond energy was generally 8–50 kJ/mol, much higher than the binding energy of hydrophobic interactions. BPA molecules would occupy the high-energy hydrogen bonding sites in priority and then extend to the low-energy hydrophobic sites. The hydrogen bonding sites effectively reduced the diffusion obstruction and promoted adsorption (Zhou et al., 2014). The involvement of hydrogen bond reduced the absolute value of ΔH and –TΔS evidently. However, the absolute value of ΔG decreased, revealing the weakened binding interactions at pH 5. The results indicated that the predominant hydrophobic interactions were lowered at acidic conditions although hydrogen bonding participated the binding interactions. At pH 5, the electrical repulsion between MPs decreased due to less negative charges of MPs interface, bringing about significant aggregation. Therefore, less binding sites were available for the hydrophobic interactions, generally presenting a lower absolute value of ΔG at pH 5.

At pH 9, the hydrophobic force was reduced owing to increased hydrophilic hydroxyl groups in BPA, leading to the decrease in the absolute values of ΔH and –TΔS. The magnified electrostatic repulsions between negatively charged MPs (Fig. 3) and BPA anions (Fig. 4) induced changes in thermodynamic parameters i.e. increased absolute value of –TΔS. What's more, hydrogen bonding was also weakened with the reduced hydrophobic force under the alkaline conditions. In aqueous solution, hydrogen bonding sites are impeded by water molecules (Zhou et al., 2014). The enhancement of hydrophilicity of BPA increased the isolation of hydrogen bonding sites by water environment, causing a lower hydrogen bond capacity. The absolute values of ΔH and –TΔS presented as the comprehensive results, that were lower than those under neutral condition.

Besides, $\pi-\pi$ bonding might also exist. It was reported that the adsorption of nano-polystyrene MPs to polychlorinated biphenyls were related with $\pi-\pi$ interactions (Velzeboer et al., 2014). However, $\pi-\pi$ interactions between BPA and polystyrene MPs might be not so obvious. The benzene rings randomly arranged on both sides of the polystyrene main chain of MPs. The limited mobility and relative displacement of polystyrene molecular chains was not convenient for BPA to diffuse into the matrix of polystyrene (Liu et al., 2019, Rochman et al., 2013). The interaction of $\pi-\pi$ bonding would induce a negative value of ΔH.

3.3. Influences of salinity and cations on the binding process

The binding process between MPs and BPA seemed independent on salinity at pH 7, with a slightly higher binding constant at 10 mM ionic strength (Table 1). Zeta potential of MPs was intimately related with the salinity (Fig. 3b). The electrical double layer of MPs was compressed with the growth of salinity, leading to reduced negative charges on MPs surface (Hu et al., 2020b). However, since BPA was in the molecular form at pH 7, the electrostatic force barely participated the binding process. Apparently, hydrophobic force and hydrogen bond are slightly influenced by the salinity of the solution. It was reported that the adsorption of three synthetic musks on MPs slightly changed with the variation of NaCl (Zhang et al., 2018b). However, salinity impacted the binding processes of several other contaminants onto MPs. In comparison to seawater, river water was conducive to the adsorption process of metals (Cd, Co, Ni and Pb) on beached plastic pellets (Holmes et al., 2014), because the competition for adsorption sites on the pellet surface between metals and divalent cations increased with the growing salinity. Increasing ionic strength was beneficial to the binding of naphthalene onto polystyrene MPs due to the improved $\pi-\pi$ interactions (Hu et al., 2020b). The increase of NaCl furthered the sorption of lubricating oil on polyethylene and polystyrene MPs owing to the outer-sphere surface complexation (Hu et al., 2017). In this work, the minor influence of salinity also implied the insignificance of $\pi-\pi$ interactions.

Table 3
Variations of zeta potential for MPs before and after binding with BPA in the presence of divalent metal ions (pH 7, 25 °C, pure water).

	Zeta potential (mV)
MPs	−3.62±0.30
MPs+1 mM $MgCl_2$	−19.91±2.08
MPs+1 mM $MgCl_2$+BPA	−20.64±0.21
MPs+1 mM $CaCl_2$	−24.40±1.27
MPs+1 mM $CaCl_2$+BPA	−20.12±1.77

Ca^{2+} and Mg^{2+} were prevalent divalent ions in water environments, which might influence the binding interactions between BPA and MPs. As shown in Table 1, Ca^{2+} and Mg^{2+} addition obviously promoted the binding process as indicated by the values of binding constants and binding sites. The presence of divalent metal ions narrowed the distance between MPs and BPA as a subtle bridge, so that the binding process became to be easier (Liu et al., 2010). Zhao et al. (2013) also documented the bridging effect of metal ions during the adsorption process of tetracycline by soil minerals. The influences of Ca^{2+} were more significant compared to those of Mg^{2+}. Addition of Ca^{2+} and Mg^{2+} increased the negative charges of MPs, especially for Ca^{2+} (Table 3). However, zeta potential of MPs became to be identical when BPA was added, indicating that Ca^{2+} had stronger capability of linking BPA to MPs surface. That might be due to the smaller fully hydrated cation diameter of Ca^{2+} (600 pm) compared to Mg^{2+} (800 pm) (Kielland 1937). Similar results were documented in other studies. Making the electrical double layer compressed and zeta potential reduced, it was found that Ca^{2+} could promote the sorption of perfluorooctanesulfonate onto polystyrene particles (Wang et al., 2015). The existences of Pb^{2+}, Cd^{2+}, and Zn^{2+} markedly enhanced the adsorption of polyethylene to tetracycline on account of the metal bridging effect (Yu et al., 2020a). Nevertheless, Ca^{2+} of high concentrations competed with 9-nitroanthrene for the adsorption sites of polypropylene and polystyrene MPs (Zhang et al., 2020). In the present work, Ca^{2+} and Mg^{2+} exerted positive effects on the binding interactions of MPs and BPA.

3.4. Environmental implications

Understanding the interaction mechanisms between BPA and MPs furthers the comprehension of the roles of MPs in the environmental fate of hydrophobic organic pollutants. With the discharge of plastic wastes into environment, plastics break down into MPs through physical, chemical and biological ways. MPs act as vectors of BPA, flowing over long distances. MPs alter the transportation and migration of BPA in aquatic environments, hence jeopardizing the aquatic ecosystems.

Environmental conditions regulate the binding strength of MPs to BPA. The binding strength is relatively higher under neutral and acidic conditions, while weaker under alkaline condition. As the pH of marine

ranges from 8.0 to 8.5, BPA that carried by MPs is more readily to be released when migrating from terrestrial water bodies to the marine environment. The results also imply that the BPA concentrations detected in marine were likely underestimated, since considerable BPA presented in the form of MPs-BPA complex. The binding strength of MPs to BPA is clearly enhanced with the increasing temperature. Therefore, BPA tends to be combined with MPs in hot seasons or areas, with the risk of BPA re-releasing into the environments in the cold seasons or areas. Divalent ions (Ca^{2+} and Mg^{2+}) promote the binding interactions between BPA and MPs, especially for Ca^{2+}. Therefore, BPA is intimately combined with MPs in water bodies of high hardness.

What's more, MPs undergo the processes of solar exposure, oxidation, thermal aging and biofilm growth in the environment, which would influence their capability of binding with the pollutants. For instance, the surface morphological changes would lower the adsorption capacity of MPs to the pollutants for the variations in specific surface area (Hüffer et al., 2018), resulting in the dynamic release of the bound pollutants. MPs degradation is not affected by biological ways fundamentally (Thompson et al., 2005), nevertheless, with the wrapping of biofilms on MPs, hydrophobic organic chemicals are readily to be enriched in microlayer (Andrady 2011). That meant MPs become mobile sources that carried with biofilm and composite pollutants, migrating in the water environments.

4. Conclusions

The binding process of BPA to MPs is solely driven by entropy, no matter under acidic, neutral or alkaline conditions. Hydrophobic forces, hydrogen bonds and electrostatic repulsions are the primary interaction mechanisms driving the binding process of polystyrene MPs to BPA. The binding strength of BPA to MPs is intimately related to pH conditions, that is higher under neutral (logK=4.96, pH 7) and acidic (logK=4.63, pH 6) conditions, while lower under alkaline condition. The dominant hydrophobic forces and hydrogen bonds are weakened, and electrostatic repulsions are magnified under alkaline condition, hence lowering the binding affinity. The binding strength pronouncedly grows with the increasing temperature from 4 to 35 ˚C. Ionic strength showed insignificant influences on the binding interaction. The presence of Ca^{2+} and Mg^{2+} is conductive to the binding process. The interactions of MPs and BPA occurs thermodynamical spontaneously, that would alter the transportation and migration of BPA pollutant in aquatic environments.

Declaration of Competing Interest

The authors declare that they have no known competing financial interests or personal relationships that could have appeared to influence the work reported in this paper.

Acknowledgments

The authors wish to thank Shanghai Key Lab for Urban Ecological Processes and Eco-Restoration (SHUES2021C01) and the Fundamental Research Funds for the Central Universities.

References

Andrady, A.L., 2011. Microplastics in the marine environment. Mar. Pollut. Bull. 62, 1596–1605.
Auta, H.S., Emenike, C.U., Fauziah, S.H., 2017. Distribution and importance of microplastics in the marine environment: a review of the sources, fate, effects, and potential solutions. Environ. Int. 102, 165–176.
Ding, L., Mao, R., Ma, S., Guo, X., Zhu, L., 2020. High temperature depended on the ageing mechanism of microplastics under different environmental conditions and its effect on the distribution of organic pollutants. Water Res. 174, 115634.
Engler, R.E., 2012. The complex interaction between marine debris and toxic chemicals in the ocean. Environ. Sci. Technol. 46, 12302–12315.
Escalona, I., de Grooth, J., Font, J., Nijmeijer, K., 2014. Removal of BPA by enzyme polymerization using NF membranes. J. Membr. Sci. 468, 192–201.
Gan, L.H., Yan, Z.R., Ma, Y.F., Zhu, Y.Y., Li, X.Y., Xu, J., 2019. Zhang, W. pH dependence of the binding interactions between humic acids and bisphenol A-A thermodynamic perspective. Environ. Pollut. 255, 113292.
Guo, X., Wang, X., Zhou, X., Kong, X., Tao, S., Xing, B., 2012. Sorption of four hydrophobic organic compounds by three chemically distinct polymers: role of chemical and physical composition. Environ. Sci. Technol. 46, 7252–7259.
Holmes, L.A., Turner, A., Thompson, R.C., 2014. Interactions between trace metals and plastic production pellets under estuarine conditions. Mar. Chem. 167, 25–32.
Hu, B., Li, Y., Jiang, L., Chen, X., Wang, L., An, S., Zhang, F., 2020a. Influence of microplastics occurrence on the adsorption of 17β-estradiol in soil. J. Hazard. Mater. 400, 123325.
Hu, E., Shang, S., Fu, Z., Zhao, X., Nan, X., Du, Y., Chen, X., 2020b. Cotransport of naphthalene with polystyrene nanoplastics (PSNP) in saturated porous media: effects of PSNP/naphthalene ratio and ionic strength. Chemosphere 245, 125602.
Hu, J.Q., Yang, S.Z., Guo, L., Xu, X., Yao, T., Xie, F., 2017. Microscopic investigation on the adsorption of lubrication oil on microplastics. J. Mol. Liq. 227, 351–355.
Hüffer, T., Weniger, A.K., Hofmann, T., 2018. Sorption of organic compounds by aged polystyrene microplastic particles. Environ. Pollut. 236, 218–225.
Jiang, Y., Li, J., Xu, S., Zhou, Y., Zhao, H., Li, Y., Xiong, C., Sun, X., Liu, H., Liu, W., Peng, Y., Hu, C., Cai, Z., Xia, W., 2019. Prenatal exposure to bisphenol a and its alternatives and child neurodevelopment at 2 years. J. Hazard. Mater. 388, 121774.
Jin, Q., Zhang, S., Wen, T., Wang, J., Gu, P., Zhao, G., Wang, X., Chen, Z., Hayat, T., Wang, X., 2018. Simultaneous adsorption and oxidative degradation of Bisphenol A by zero-valent iron/iron carbide nanoparticles encapsulated in N-doped carbon matrix. Environ. Pollut. 243, 218–227.
Kielland, J., 1937. Individual activity coefficients of ions in aqueous solutions. J. Am. Chem. Soc. 59, 1675–1678.
Lei, L.L., Wu, S.Y., Lu, S.B., Liu, M.T., Song, Y., Fu, Z.H., Shi, H.H., Raley-Susman, K.M., He, D.F., 2018. Microplastic particles cause intestinal damage and other adverse effects in zebrafish Danio rerio and nematode Caenorhabditis elegans. Sci. Total Environ. 619, 1–8.
Li, Y., Li, M., Li, Z., Yang, L., Liu, X., 2019. Effects of particle size and solution chemistry on Triclosan sorption on polystyrene microplastic. Chemosphere 231, 308–314.
Liu, L., Fokkink, R., Koelmans, A.A., 2016. Sorption of polycyclic aromatic hydrocarbons to polystyrene nanoplastic. Environ. Toxicol. Chem. 35, 1650–1655.
Liu, L., Gao, D.W., Zhang, M., Fu, Y., 2010. Comparison of Ca^{2+} and Mg^{2+} enhancing aerobic granulation in SBR. J. Hazard. Mater. 181, 382–387.
Liu, W., Zhang, J., Liu, H., Guo, X., Zhang, X., Yao, X., Cao, Z., Zhang, T., 2021. A review of the removal of microplastics in global wastewater treatment plants: characteristics and mechanisms. Environ. Int. 146, 106277.
Liu, X., Shi, H., Xie, B., Dionysiou, D.D., Zhao, Y., 2019. Microplastics as both a sink and a source of bisphenol a in the marine environment. Environ. Sci. Technol. 53, 10188–10196.
Liu, X., Wang, J., 2020. Algae (Raphidocelis subcapitata) mitigate combined toxicity of microplastic and lead on Ceriodaphnia dubia. Front. Environ. Sci. Eng. 14, 97.
Luo, H., Liu, C., He, D., Xu, J., Sun, J., Li, J., Pan, X., 2022. Environmental behaviors of microplastics in aquatic systems: a systematic review on degradation, adsorption, toxicity and biofilm under aging conditions. J. Hazard. Mater. 423, 126915.
Rochman, C.M., Manzano, C., Hentschel, B.T., Simonich, S.L.M., Hoh, E., 2013. Polystyrene plastic: a source and sink for polycyclic aromatic hydrocarbons in the marine environment. Environ. Sci. Technol. 47, 13976–13984.
Ross, P.D., Subramanian, S., 1981. Thermodynamics of protein association reactions: forces contributing to stability. Biochemistry 20, 3096–3102.
Thompson, R., Moore, C., Andrady, A., Gregory, M., Takada, H., Weisberg, S., 2005. New directions in plastic debris. Science 310, 1117.
Velzeboer, I., Kwadijk, C., Koelmans, A.A., 2014. Strong sorption of PCBs to nanoplastics, microplastics, carbon nanotubes, and fullerenes. Environ. Sci. Technol. 48, 4869–4876.
Wang, F., Shih, K.M., Li, X.Y., 2015. The partition behavior of perfluorooctanesulfonate (PFOS) and perfluorooctanesulfonamide (FOSA) on microplastics. Chemosphere 119, 841–847.
Wang, F., Wong, C.S., Chen, D., Lu, X.W., Wang, F., Zeng, E.Y., 2018. Interaction of toxic chemicals with microplastics: a critical review. Water Res. 139, 208–219.
Wang, T., Yu, C., Chu, Q., Wang, F., Lan, T., Wang, J., 2020. Adsorption behavior and mechanism of five pesticides on microplastics from agricultural polyethylene films. Chemosphere 244, 125491.
Wang, W., Wang, J., 2018. Comparative evaluation of sorption kinetics and isotherms of pyrene onto microplastics. Chemosphere 193, 567–573.
Wu, P.F., Cai, Z.W., Jin, H.B., Tang, Y.Y., 2019. Adsorption mechanisms of five bisphenol analogues on PVC microplastics. Sci. Total Environ. 650, 671–678.
Yan, Z.R., Zhu, Y.Y., Meng, H.S., Wang, S.Y., Gan, L.H., Li, X.Y., Xu, J., Zhang, W., 2019. Insights into thermodynamic mechanisms driving bisphenol A (BPA) binding to extracellular polymeric substances (EPS) of activated sludge. Sci. Total Environ. 677, 502–510.
Yang, K., Wu, W., Jing, Q., Zhu, L., 2008. Aqueous adsorption of aniline, phenol, and their substitutes by multi-walled carbon nanotubes. Environ. Sci. Technol. 42, 7931–7936.
Yu, F., Yang, C., Huang, G., Zhou, T., Zhao, Y., Ma, J., 2020a. Interfacial interaction between diverse microplastics and tetracycline by adsorption in an aqueous solution. Sci. Total Environ. 721, 137729.
Yu, J., Xiao, K., Xue, W., Shen, Y.-x., Tan, J., Liang, S., Wang, Y., Huang, X., 2020b. Excitation-emission matrix (EEM) fluorescence spectroscopy for characterization of organic matter in membrane bioreactors: principles, methods and applications. Front. Environ. Sci. Eng. 14, 31.
Zhang, H., Wang, J., Zhou, B., Zhou, Y., Dai, Z., Zhou, Q., Chriestie, P., Luo, Y., 2018a. Enhanced adsorption of oxytetracycline to weathered microplastic polystyrene: kinetics, isotherms and influencing factors. Environ. Pollut. 243, 1550–1557.

Zhang, J., Chen, H., He, H., Cheng, X., Ma, T., Hu, J., Yang, S., Li, S., Zhang, L., 2020. Adsorption behavior and mechanism of 9-nitroanthracene on typical microplastics in aqueous solutions. Chemosphere 245, 125628.
Zhang, X.J., Zheng, M.G., Wang, L., Lou, Y.H., Shi, L., Jiang, S.J., 2018b. Sorption of three synthetic musks by microplastics. Mar. Pollut. Bull. 126, 606–609.
Zhao, Y., Tan, Y., Guo, Y., Gu, X., Wang, X., Zhang, Y., 2013. Interactions of tetracycline with Cd (II), Cu (II) and Pb (II) and their cosorption behavior in soils. Environ. Pollut. 180, 206–213.
Zhou, X.Y., Wei, J.F., Liu, K., Liu, N.N., Zhou, B., 2014. Adsorption of bisphenol a based on synergy between hydrogen bonding and hydrophobic interaction. Langmuir 30, 13861–13868.